

Frequency domain analysis of Froude-Krylov and diffraction forces on TLP

Ebrahim Malayjerdi¹ and Mohammad Reza Tabeshpour^{*2}

¹Mechanical Engineering Department, Sharif University of Technology, Tehran, Iran

²Mechanical Engineering Department, Center of Excellence in Hydrodynamics and Dynamics of Marine Vehicles, Sharif University of Technology, Tehran, Iran

(Received April 28, 2016, Revised August 28, 2016, Accepted August 30, 2016)

Abstract. Tension Leg Platform (TLP) is a floating structure that consists of four columns with large diameter. The diffraction theory is used to calculate the wave force of floating structures with large dimensions (TLP). In this study, the diffraction and Froude-Krylov wave forces of TLP for surge, sway and heave motions and wave force moment for roll, pitch degrees of freedom in different wave periods and three wave approach angles have been investigated. From the numerical results, it can be concluded that the wave force for different wave approach angle is different. There are some humps and hollows in the curve of wave forces and moment in different wave periods (different wavelengths). When wave incidents with angle 0 degree, the moment of diffraction force for pitch in high wave periods (low frequencies) is dominant. The diffraction force for heave in low wave periods (high wave frequencies) is dominant. The phase difference between Froude-Krylov and diffraction forces is important to obtain total wave force.

Keywords: TLP; hydrodynamic; wave forces; diffraction; Froude-Krylov; phase difference

1. Introduction

TLP hull is similar to semisubmersible platform. Vertically small motions and high stability, low cost increases rate as increasing depth in comparison to other types of platforms, capability of production from deep seas are some advantages of TLPs. The disadvantages are: high cost subsea foundation installation, sensitive fatigue damage in tethers, tether connections repair and maintenance difficulty, low capacity storage tanks. There are important conceptual problems in dynamic analysis of such structures (Tabeshpour and Malayjerdi 2016).

The Morison equation is used to estimate the wave loads in the design of oil platforms and other offshore structures (Gudmestad *et al.* 1996, Veritas *et al.* 2005). This equation is used when the diameter of the cylinder is much smaller than the wavelength. If the diameter of the body is not small compared to the wavelength, diffraction effects have to be taken into account (Chaplin. 1984). Zeng *et al.* (2007) investigated 6-DOF coupled motions, time history of motions and wetted area, free surface and viscous drag effect and dynamic analysis of ISSC TLP in depth of 415 m in regular sea. Anitha *et al.* (2010) presented a new geometric configuration that could be a better

*Corresponding author, Dr., E-mail: tabeshpour@yahoo.com

alternative to an existing configuration. Also in this paper a three-column mini TLP is designed and added mass, radiation damping, transfer functions of wave force and RAOs of motions is investigated for three column mini TLP and compared with an existing four column mini TLP. Tabeshpour *et al.* (2013) and (2006) developed hydrodynamic analysis of heave and pitch motions of tension leg platforms. They presented an exact solution for heave and pitch vibrations of a TLP interacting with ocean wave. Wu *et al.* (2014) investigated the influence of the legs underwater on the hydrodynamic response of the multi-leg floating structure. Also, they studied the hydrodynamic responses of the structure in different cases numerically simulated by applying the three-dimensional potential theory. The hydrodynamic coefficients, wave excitation loads and RAOs of the six degrees of freedom in different wave frequencies were calculated and compared. Yang *et al.* (2012) studied a coupled dynamic analysis for wave interaction with a truss spar and its mooring line/riser system in the time domain and developed a time domain second order method to estimate of hydrodynamic loads. They also developed a higher-order boundary element method to calculate the velocity potential of the resulting flow field at each time step. Drake (2011) presented an analytical solution for the horizontal drift force acting on a uniform circular cylinder that is undergoing surge and pitch motion in regular waves. Ghadimi *et al.* (2012) studied an analytical solution of the diffraction problem for a cylinder of particular radius (α) floating in a channel of specific depth (d). Kunisu (2010) evaluated wave force of the submerged floating tunnel based on the diffraction theory by Boundary Element Method and the Morison's equation. Also, the numerical results of the theories compared with experimental results.

In this study deals with estimating of the Froude-Krylov, diffraction and total forces on TLP induced by regular wave in the frequency domain. The numerical simulations are based on the Boundary Element Method (BEM) to compute the forces. TF^* and phase of wave forces for incident angle 0 degree are illustrated and importance of phase difference between Froude-Krylov and diffraction are also examined. Spectral analysis of wave forces in three wave approach angles (0, 45 and 90 degree) is done, then root mean square (RMS) of the wave forces PSD^\dagger are estimated and compared.

2. Diffraction, Froude-Krylov and radiation wave forces

In This section, the hydrodynamic fluid loading of diffracting bodies in regular waves is explained. The fluid is assumed to be ideal and non-rotational to use potential theory. Velocity potential is defined as follows (Tabeshpour and Malayjerdi 2016)

$$\phi(x, y, z, t) = \phi(x, y, z) e^{-i\omega t} \quad (1)$$

Where ϕ is complex potential function and is separated into radiation waves due to the six modes of body motion, the incident wave and diffracted wave, and ω is frequency of incident wave and is expressed as follow

$$\phi(x, y, z, t) = \phi_R + \phi_I + \phi_D \quad (2)$$

* Transfer Function

† Power Spectral Density

Where ϕ_R, ϕ_I and ϕ_D represent radiation, incident wave and diffracted wave potential.

Two problems for the body are considered to obtain ϕ . The first problem is related to the floating body undergoing harmonic oscillation in still water. The body motions will cause radiation force to create. The second problem is regarding fixed body subjected to regular wave. Froude-Krylove and diffraction forces are components of wave forces acted to fixed the body. Therefore, the total potential can be written as below

$$\phi(x, y, z, t) e^{-i\omega t} = [(\phi_I + \phi_D) + \sum_{j=1}^6 \phi_j x_j] e^{-i\omega t} \tag{3}$$

where $\phi_I, \phi_d, \phi_j, x_j$ are incident wave potential, diffracted wave potential, radiation potential due to j th motion (per unit wave amplitude), respectively. The wave form and the associated velocity potential are given as follows (Tabeshpour *et al.* 2013)

$$\eta_i = -iA_i e^{-i\omega t} \tag{4}$$

$$\phi_I = \frac{A_i g}{\omega} \frac{\cos(K_1(z+h))}{\cos(K_1 h)} e^{-i\omega t} \tag{5}$$

Where A_i is the amplitude incident wave, g is acceleration of gravity, h is the water depth, and $K_1 = -ik$, where $k = 2\pi / L$ is the wave number with L as the wavelength. K_1 satisfies the dispersion relation (Tabeshpour *et al.* 2013)

$$\omega^2 = g K_1 \tanh(K_1 h) \tag{6}$$

By solving the Laplace equation, Potential functions for incompressible, non-viscose and irreversible flows are obtained

$$\nabla^2 \phi = 0 \quad \text{or} \quad \frac{\partial^2 \phi}{\partial x^2} + \frac{\partial^2 \phi}{\partial y^2} + \frac{\partial^2 \phi}{\partial z^2} = 0 \tag{7}$$

Also concurrent with solution of Laplace equation, boundary conditions must be satisfied. Boundary conditions are as follows

free surface boundary condition

$$\tau_\omega = g \frac{\partial \phi}{\partial z} - \omega^2 \phi = 0 \tag{8}$$

bottom boundary condition

$$u = \frac{\partial \phi}{\partial z} = 0 \text{ in } z = -h \tag{9}$$

Kinematic boundary condition

$$\frac{\partial \phi}{\partial n} = \vec{v} \cdot \vec{n} \tag{10}$$

where \vec{n} is normal vector to surface and Sommerfeld boundary condition is as follow

$$|\nabla\phi| \rightarrow 0 \quad \text{when } r \rightarrow -\infty \quad (11)$$

Where $r = \sqrt{x^2 + y^2 + z^2}$, τ_w is shear stress of fluid. When the potential functions are known, the first order hydrodynamic pressure distribution can be calculated using the linearized Bernoulli equation

$$p = -\rho \frac{\partial\phi}{\partial t} \quad (12)$$

The fluid forces are computed by integrating the pressure over the wetted surface of the body as follows

$$F_{w_j} = - \int_s i \omega \rho (\phi_I + \phi_D) n_j ds \quad (13)$$

Where F_{w_j} is the wave force in j -the direction, n_j is the generalized surface normal for j -th direction and s is the wetted surface of the body in equilibrium position. The diffraction and Froude-Krylov forces are found as follows

$$F_{D_j} = - \int_s i \omega \rho (\phi_D) n_j ds \quad (14)$$

$$F_{I_j} = - \int_s i \omega \rho (\phi_I) n_j ds \quad (15)$$

Where F_{D_j} and F_{I_j} are diffraction and Froude-Krylov forces respectively. Also diffraction and Froude-Krylov forces in the surge and heave directions are estimated by integration of the fluid pressure around the body in the x and z directions, respectively. The total wave exciting forces can then be estimated by summing two the force components (The Froude-Krylov and diffraction forces). The Froude-Krylov and diffraction forces are generated due to undistributed and distributed waves, respectively. The total Moments of diffraction and Froude-Krylov forces can be expressed as below

$$\sum \vec{M} = \int_A \rho (\phi_I + \phi_D) n_j \times \vec{r} ds \quad (16)$$

Where \vec{M} is moment vector and \vec{r} is the place vector of element of body respect to the region, which is located in the center of flotation.

The roll and pitch exciting moments of diffraction and Froude-Krylov forces can be expressed as follows

$$\begin{aligned} M_{I_4} &= F_{I_2} z_c + F_{I_3} y_c \\ M_{d_4} &= F_{d_2} z_c + F_{d_3} y_c \end{aligned} \quad (17)$$

$$\begin{aligned} M_{I_5} &= F_{I_1} z_c + F_{I_3} x_c \\ M_{d_5} &= F_{d_1} z_c + F_{d_3} x_c \end{aligned} \quad (18)$$

M_{I_4} and M_{I_5} express moment of Froude-Krylov force for roll and pitch motions. M_{d_4} and M_{d_5} are moment of diffraction force for roll and pitch motions, respectively. F_{I_1} , F_{I_2} and F_{I_3} are Froude-Krylov force for surge, sway and heave motions, respectively. F_{d_1} , F_{d_2} and F_{d_3} are diffraction forces for surge, sway and heave motions, respectively. x_c , y_c and z_c are distance between the wave force and center of gravity of TLP in surge, sway and heave directions, respectively.

3. Frequency domain analysis

In this study, for determining of energy of wave force in wave frequencies, spectral analysis has been carried out. For a linear system, PSD of wave force in a wave frequency is obtained by multiplying the square of the wave force transfer function with PSD of wave elevation and can be written as follows

$$S_F(\omega) = |TF_F(\omega)|^2 S_\zeta(\omega) \quad (19)$$

Where, $S_F(\omega)$ and $S_\zeta(\omega)$ are PSD of wave force and wave elevation. $TF_F(\omega)$ is a TF of wave force. The target PSD of wave for the numerical study in this study is assumed JONSWAP and for $H_s = 8m$ is plotted in Fig. (1).

Numerical results of wave forces and moment (Froude-Krylov and diffraction) in frequency domain for surge, sway, heave, roll and pitch motions when wave incidents with wave approach angles 0, 45 and 90 degree are illustrated in this section. The case study is a tension-leg platform named ISSC TLP and the specifications are given in table (1), (Zeng *et al.* 2007):

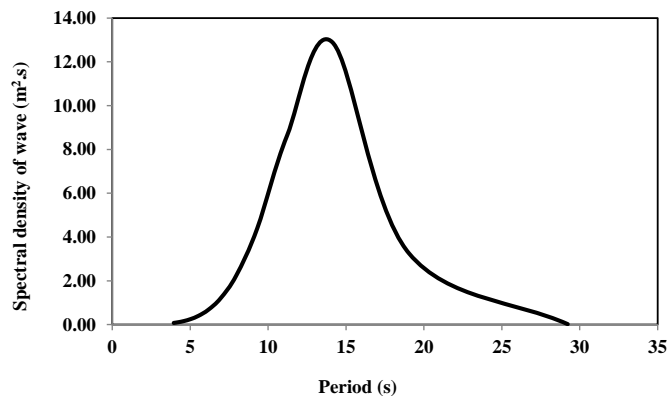


Fig. 1 Spectral density of wave

Table 1 specifications of ISSC TLP in depth of 230 m

Draft	35m	External radius of tendon	0.3m
Displacement	$54.5 \times 10^6 \text{ kg}$	Internal radius of tendon	0.212m
Mass	$40.5 \times 10^6 \text{ kg}$	Length of tendon	195
Roll motion moment of inertia	$82.37 \times 10^9 \text{ kg m}^2$	Pre-tension in tendon	1.1445E7 N
Pitch motion moment of inertia	$82.37 \times 10^9 \text{ kg m}^2$	Young's modulus of tendon	$2.1E11 \text{ N/m}^2$
yaw motion moment of inertia	$98.07 \times 10^9 \text{ kg m}^2$	Axial stiffness of tendon	$1.5E8 \text{ N/m}$
Center of gravity height	38m	Number of tendons under leg	3

Fig. 2(a) shows TF of Froude-Krylov, diffraction and total wave forces on TLP for surge and Fig. 2(b) illustrates phase of wave forces for surge, when wave incidents with wave approach angle 0 degree. It can be seen that Froude-Krylov force for surge in the region I ($4s \leq \text{wave period} < 6s$) is dominant. In the region II ($11s \leq \text{wave period} \leq 19s$), diffraction force is dominant and Froude-Krylov and diffraction forces approximately are same in the region III ($6s \leq \text{wave period} \leq 9.5s$). There are some humps and hollows in the curve of wave forces of TLP in surge and they occur simultaneously. The global shapes of both Froude-Krylov and diffraction forces are similar. At wave period 8 s, phase difference among Froude-Krylov and diffraction forces is low. Therefore, in curve of total force that is the sum of Froude-Krylov and diffraction forces, occurs a hump. The phase difference at wave period 5 s, approximately is 120 degrees. It causes that total force is equal to Froude-Krylov.

Fig. 3(a) presents TF of wave forces of TLP for heave degree of freedom in frequency domain when wave approach angle is 0 degree. It is clear that the Froude-Krylov wave force is insignificant rather than diffraction force in the regions I ($5s \leq \text{wave period} \leq 8s$) and II ($11s \leq \text{wave period} \leq 14s$) and diffraction force is dominant in this region. At wave period 8s and 14 s, the diffraction wave force is greater than total wave force because the phase difference between Froude-Krylov and diffraction forces is approximately 180 degrees. Also, at wave period 19 s, the phase difference is 180 degrees and it causes Froude-Krylov force to be more than from the total force. At wave period 11.2 s, phase difference is low and it leads the total force to be greater than Froude-Krylov and diffraction forces. At wave periods 9.3 and 19 s, Froude-Krylov force is dominant.

Also by comparing Figs. 2(a) and 3(a), it can be concluded that wave force for surge very greater than heave force. At some wave periods the humps and hollows of diffraction force differ with Froude-Krylov force in heave, but for surge, they occur simultaneously.

The diffraction, Froude-Krylov and total moment of forces in pitch degree of freedom when wave approach angle is 0 degree is shown in Fig. 4(a). The pitch moment is created due to the wave forces in surge and heave motions (see Eqs. (12) and (13)). From Figs. 2(a) and 4(a), it is clear that at wave period 8 s in the curves of wave force and moment for surge and pitch occurs hump and at wave period 6 s occurs hollows on the both of them. The humps and hollows of pitch

moment and the wave force of surge happen in the same wave periods. In addition, it is seen that the moment of diffraction force for pitch in high wave period (low frequencies) is dominant. Fig. 4 (b) illustrates phase of wave force moment in pitch direction. At wave period 8s, the phase difference between Froude-Krylov and diffraction forces are low and causes in TF of total moment occurs hump. At wave period 9.3 s, the phase difference is approximately 180 degrees and it leads Froude-Krylov moment to be greater than from total moment.

From Figs. 2(b), 3(b) and 4(b), it is clear that the phase difference between Froude-Krylov and diffraction forces for surge and pitch directions is low in high wave periods but it is high for heave direction.

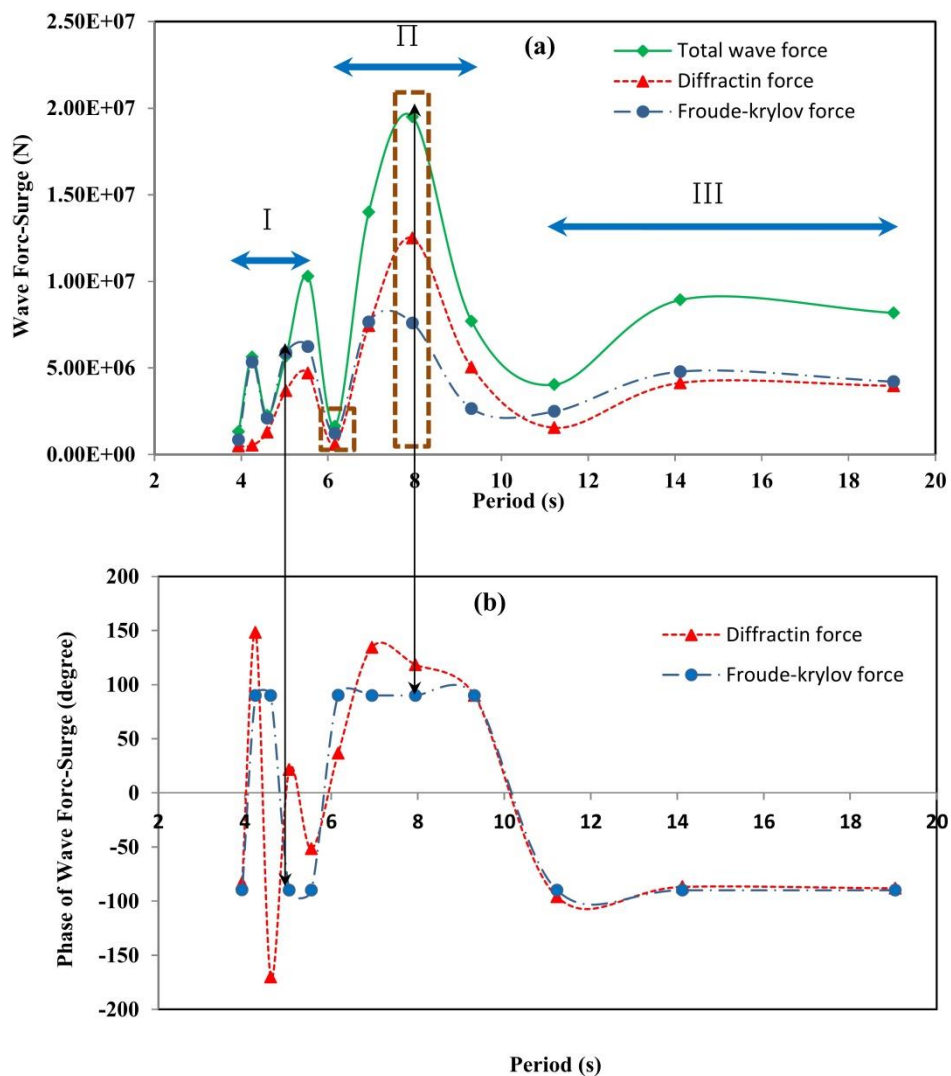


Fig. 2 (a) Wave forces of TLP for surge degree of freedom and (b) Phase of wave forces for surge, wave approach angle is 0 degree

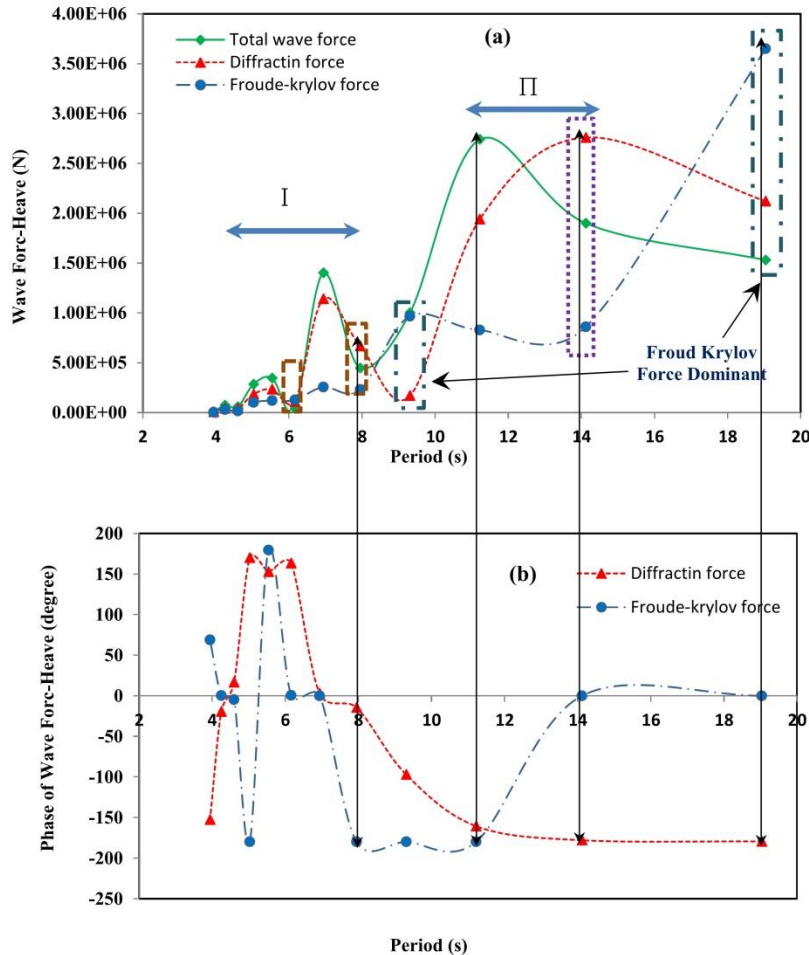


Fig. 3 (a) The wave forces of TLP for heave degree of freedom and (b) The phase of wave force for heave, wave approach angle is 0 degree

Fig. 5(a) shows RMS of wave forces PSD for surge motion. From Fig. 5(a), it is clear that wave force for surge is significant when a wave incident with angle 0 degree but is insignificant when wave approach angle is 90 degrees. It is seen that diffraction and Froude-Krylov forces are approximately equal for surge. The wave force for surge when wave approach angle is 0 degree is approximately two times as much as rather than wave approach angle is 45 degree. The RMS of wave forces PSD for sway motion is shown in Fig. 5(b). From Fig. 5(b), it is clear that when wave incidents with angle 90 degrees, wave force for sway is significantly greater than 45 and 0 degrees. The RMS of wave forces PSD for heave motion is shown in Fig. 5(c). It can be seen that the Froude-Krylov force of heave are equal in three wave approach angles. The diffraction force is greater than total force for heave in three wave approach angle because PSD of wave in the range of wave periods 12-16 s is dominant and TF of diffraction wave force for heave is dominant in this range.

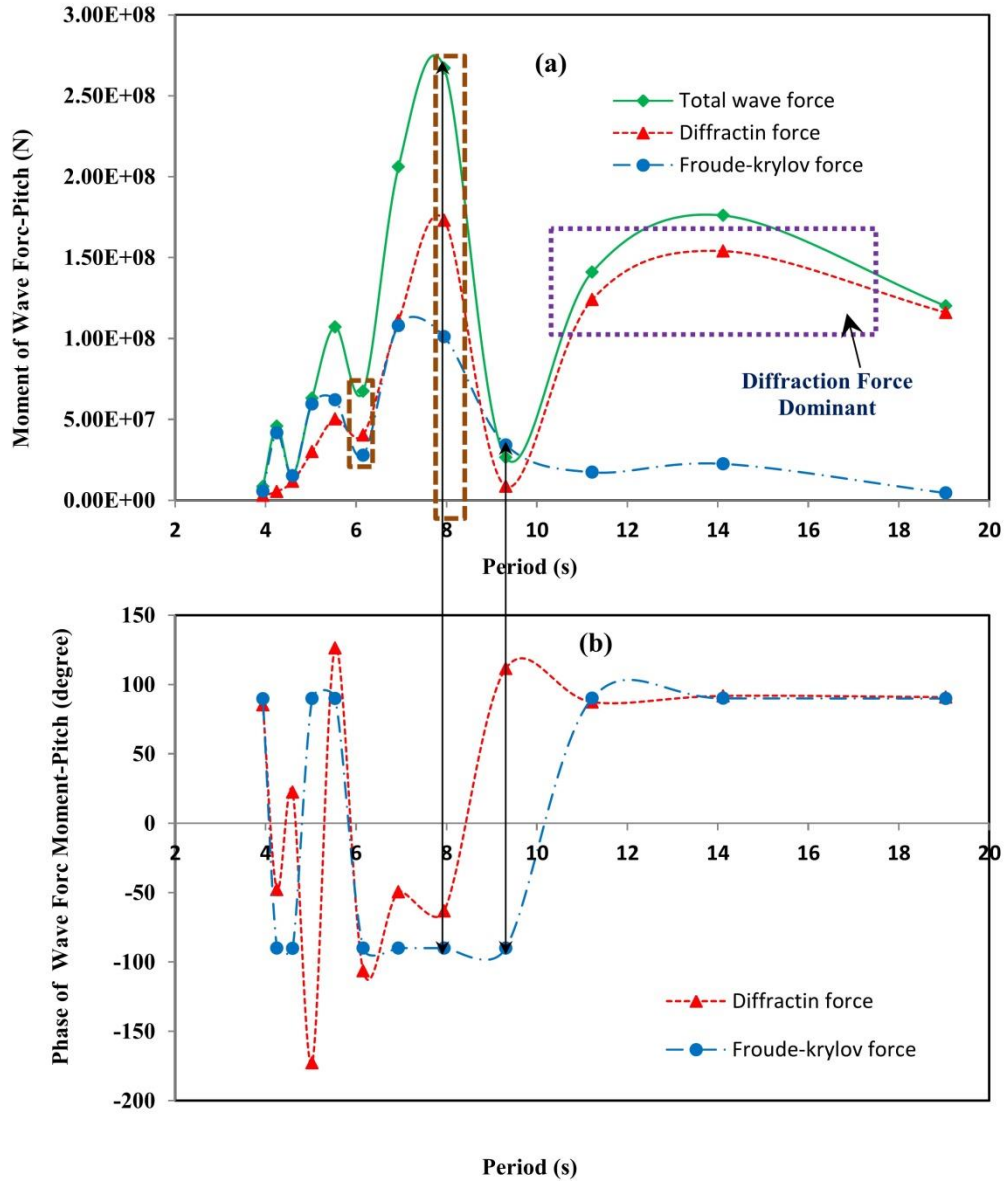


Fig. 4 (a) moments of force for pitch degree of freedom and (b) Phase of wave force moment, wave approach angle is 0 degree

Figs. 6(a) and 6(b) illustrate RMS of moment of wave force for roll and pitch rotations respectively. From Figs. 6(a) and 6(b), it is seen that moment of Froude-Krylov force for roll and pitch is insignificant. When wave approach angle is 90 degrees moment of wave force for roll is greater than when wave approach angle is 45 degrees. The diffraction moment constitutes the greater portion of the total moment for roll and pitch.

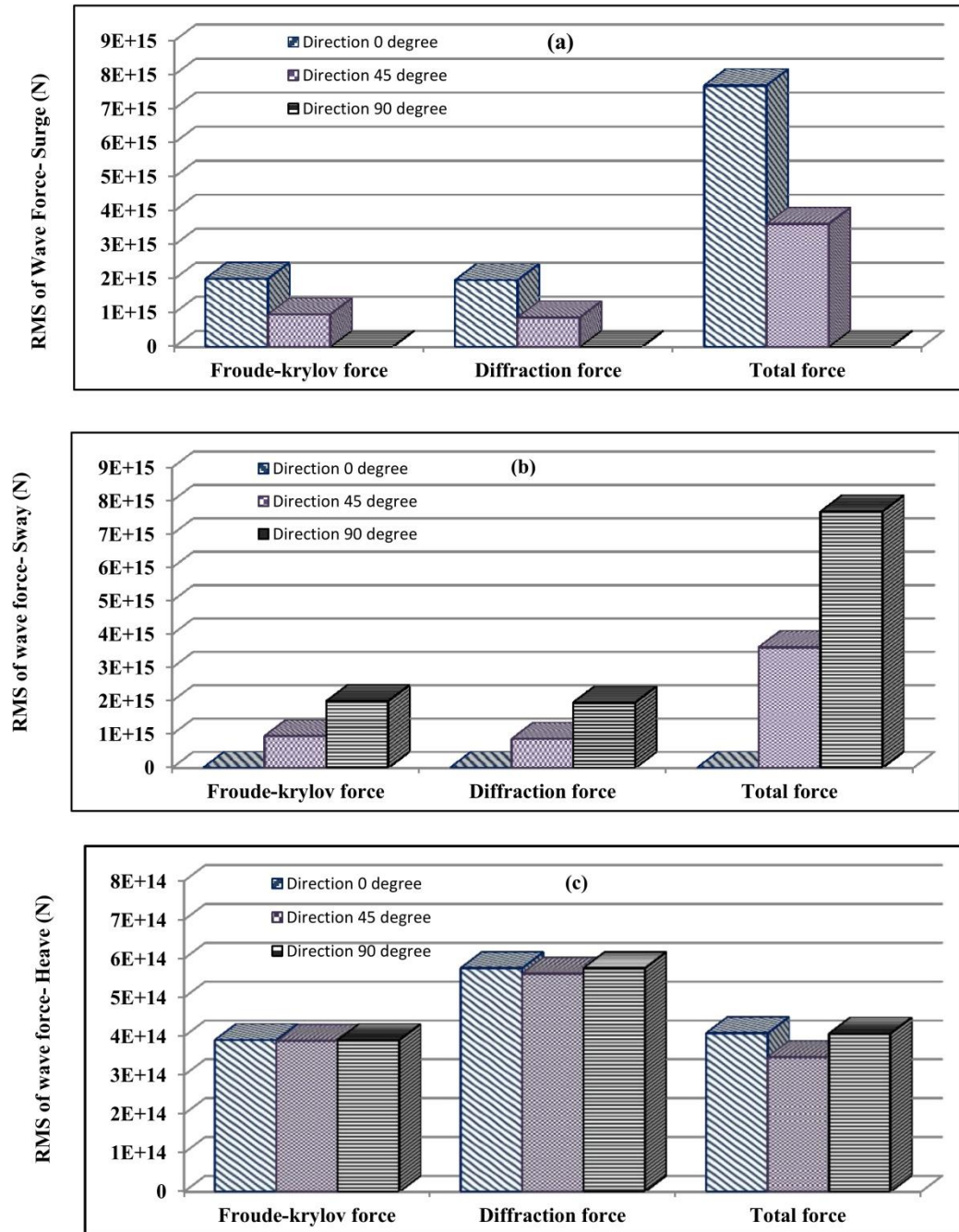


Fig. 5 (a) RMS of the wave force for surge, (b) RMS of the wave force for sway and (c) RMS of the wave force for heave

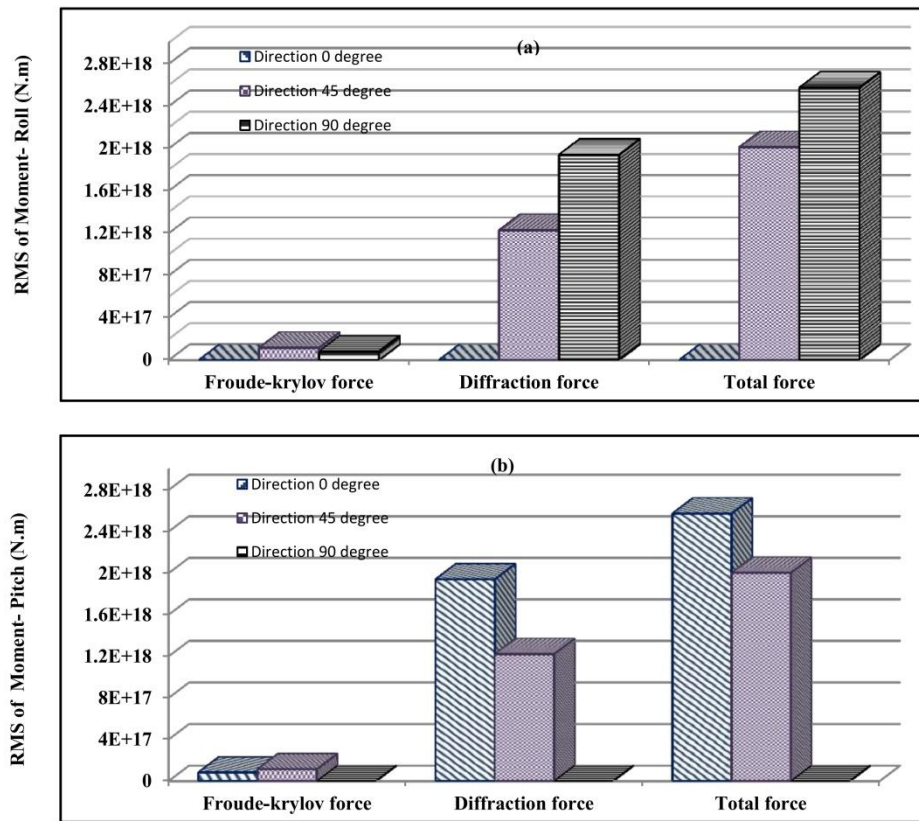


Fig. 6 (a) RMS of the wave force moment for roll and (b) RMS of the wave force moment for pitch

4. Conclusions

In this study hydrodynamic analysis of TLP is conducted by Boundary Element Method (BEM). The diffraction and Froude-Krylov wave forces for surge, sway, heave and moments for roll and pitch in three wave approach angle (0, 45 and 90 degrees) are investigated. From the numerical results, some points are reported as follows:

There are some humps and hollows in curve of wave forces and moment. The hollows and humps occur in different wave periods (different wavelengths). The hollows and humps of Froude-Krylov and diffraction wave force for surge and wave force moment for pitch approximately occur simultaneously, but these hollows and humps for heave differ with together.

When wave incidents with angle 0 degree, the moment of diffraction force for pitch in high wave periods (low frequencies) is dominant. The diffraction force for heave in low wave periods (high wave frequencies) is dominant. The wave force of TLP for surge direction is very greater than heave direction. The diffraction and Froude-Krylov forces are approximately equal for surge. The phase difference of Froude-Krylov and diffraction forces is important to obtain total wave force because when it is high (180 degree), the total force is lower than diffraction or Froude-

Krylov forces and when the phase is low, higher total force is created.

When the wave approach angle is 45 degrees, the wave forces for surge and sway and the moment of wave force for roll and pitch motions are equal. When the wave approach angle is 90 degree, the wave force for sway is significant but for surge is insignificant. The Froude krylov and diffraction force for heave direction in three wave approach angles are approximately the same. The moment of Froude-Krylov force for roll and pitch is insignificant. The diffraction moment constitutes the greater portion of the total moment for roll and pitch.

References

- Chaplin, J.R. (1984), "Nonlinear forces on a horizontal cylinder beneath waves", *J. Fluid Mech.*, **147**, 449-464.
- Drake, K.R. (2011), "An analytical approximation for the horizontal drift force acting on a deep draught spar in regular waves", *Ocean Eng.*, **38**(5), 810-814.
- Ghadimi, P., Bandari, H.P. and Rostami, A.B. (2012), "Determination of the heave and pitch motions of a floating cylinder by analytical solution of its diffraction problem and examination of the effects of geometric parameters on its dynamics in regular waves", *Int. J. Appl. Math. Res.*, **1**(4), 611-633.
- Gudmestad, O.T and Moe, G. (1996), "Hydrodynamic coefficients for calculation of hydrodynamic loads on offshore truss structures", *Mar. Struct.*, **9**(8), 745-758.
- Joseph, A., Mangal, L. and George, P.S. (2010), "Coupled dynamic response of a three-column mini TLP", *J. Naval Architect. Marine Eng.*, **6**(2), 52-61.
- Kunisu, H. (2010), "Evaluation of wave force acting on submerged floating tunnels", *Procedia Eng.*, **4**, 99-105.
- Tabeshpour, M.R. and Malayjerdi, E. (2016), "Investigation of the pitch motion portion in vertical response at sides of TLP", *J. Marine Sci. Appl.*, **15**(2), 1-7.
- Tabeshpour, M.R., Ataie Ashtiani, B., Seif, M.S. and Golafshani, A.A. (2013), "Hydrodynamic damped pitch motion of tension leg platforms", *Int. J. Marine Sci. Eng.*, **3**(2), 91-98.
- Tabeshpour, M.R., Golafshani, A.A., Ashtiani, B.A. and Seif, M.S. (2006), "Analytical solution of heave vibration of tension leg platform", *J. Hydrology Hydromech.*, **54**(3), 280-289.
- Veritas, D.N. (2005), Guidelines on design and operation of wave energy converters, Carbon Trust.
- Wu, H.L., Chen, X.J., Huang, Y.X. and Wang, B. (2014), "Influence of the legs underwater on the hydrodynamic response of the multi-leg floating structure", *Ships Offshore Struct.*, **9**(6), 578-595.
- Yang, M., Teng, B., Ning, D. and Shi, Z. (2012), "Coupled dynamic analysis for wave interaction with a truss spar and its mooring line/riser system in time domain", *Ocean Eng.*, **39**, 72-87.
- Zeng, X.H., Shen, X.P. and Wu, Y.X. (2007), "Governing equations and numerical solutions of tension leg platform with finite amplitude motion", *Appl. Math. Mech.*, **28**, 37-49.